CORE
Metadata, citation and similar papers at core.ac.uk
Provided by Edinburgh Research Explorer

THE UNIVERSITY of EDINBURGH

Edinburgh Research Explorer

Analysis of Autoinduction, Inhibition, and Autoinhibition in a Rh-Catalyzed C-C Cleavage

Citation for published version:
Keske, E, West, T & Lloyd-jones, GC 2018, 'Analysis of Autoinduction, Inhibition, and Autoinhibition in a Rh-Catalyzed C-C Cleavage: Mechanism of Decyanative Aryl Silylation', ACS Catalysis, vol. 8, no. 9, pp. 8932-8940. https://doi.org/10.1021/acscatal.8b02809

Digital Object Identifier (DOI):
10.1021/acscatal.8b02809

Link:
Link to publication record in Edinburgh Research Explorer

Document Version:
Peer reviewed version

Published In:
ACS Catalysis

General rights
Copyright for the publications made accessible via the Edinburgh Research Explorer is retained by the author(s) and / or other copyright owners and it is a condition of accessing these publications that users recognise and abide by the legal requirements associated with these rights.

Take down policy
The University of Edinburgh has made every reasonable effort to ensure that Edinburgh Research Explorer content complies with UK legislation. If you believe that the public display of this file breaches copyright please contact openaccess@ed.ac.uk providing details, and we will remove access to the work immediately and investigate your claim.

Download date: 12. Sep. 2019

Analysis of Auto-Induction, Inhibition and Auto-Inhibition in a Rh-Catalyzed C-C Cleavage: Mechanism of Decyanative Aryl-Silylation

Eric C. Keske, Thomas H. West, and Guy C. Lloyd-Jones*

EaStChem, School of Chemistry, University of Edinburgh, Joseph Black Building, David Brewster Road, Edinburgh, EH9 3FJ, United Kingdom.

KEYWORDS Rhodium, C-C bond Activation, Disilanes, Induction, Isotopic Labelling, Autoinduction, Kinetics, Isonitriles

ABSTRACT: The mechanism the Chatani-Tobisu rhodium-catalyzed decyanative silylation of aryl nitriles by hexamethyldisilane (Me_3Si-$SiMe_3$) has been investigated by *in-situ* NMR spectroscopy. The production of Ar-$SiMe_3$ evolves in three distinct phases: slow catalyst induction is followed by a period of rapidly-accelerating turnover, and then, after approximately three catalyst turnovers, the onset of progressive inhibition. The processes giving rise to these phenomena have been elucidated by isotopic labelling ($^{13}C/^{15}N$) and kinetic analysis, and it is shown that, in addition to facilitating catalyst turnover to generate Ar-$SiMe_3$, the reactants serve other roles. Me_3Si-$SiMe_3$ functions as a slow exogenous precatalyst activator, and as a moderately powerful catalyst inhibitor. In contrast ArCN acts as a precatalyst inhibitor. Moreover, the co-product from the reaction (trimethylsilyl cyanide, Me_3SiCN), acts as a powerful endogenous precatalyst activator and catalyst inhibitor, together giving rise to sigmoidal temporal concentration profiles for [Ar-$SiMe_3$]. Kinetic studies of the reaction during the phase of progressive inhibition suggest that, for a given initial catalyst concentration, the maximum rate of turnover is achieved when the concentration of [Me_3Si-$SiMe_3$] and [ArCN] partition the Rh equally between two major resting states, one on-cycle, the other off-cycle. The off-cycle resting-state was identified as a Rh(III) complex: $(Me_3Si)_3Rh(CN\text{-}SiMe_3)_3$, as confirmed by independent synthesis and isotopic labelling ($^{13}C/^{15}N$); the on-cycle resting state has been tentatively assigned as $(Me_3Si\text{-}NC)_3RhAr$. Overall the results indicate that the catalytic process can in principle be made much more efficient by engendering a pathway or process for Me_3SiCN sequestration.

Introduction

The cleavage ('activation') of C-C σ-bonds by transition metals remains a significant challenge in synthetic chemistry.[1] In contrast to the more commonly encountered C-H activation, there have been far fewer reports on the successful cleavage of C-C bonds with homogeneous catalysts.

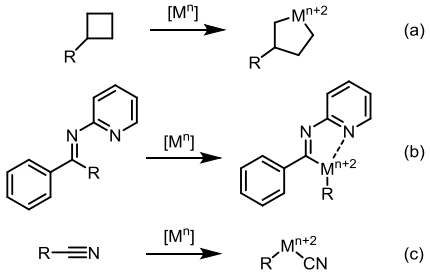

Scheme 1. Examples of Metal-mediated C-C Bond Cleavage

Most metal-catalyzed C-C σ-bond cleaving processes proceed via pathways involving the oxidative addition of compounds containing strained rings,–directing groups, or polarized C-C bonds such as organonitriles (Scheme 1, a-c).[2] As such, these reactions commonly feature low-valent and electron-rich transition metal catalysts. An interesting example of transition metal mediated C-C σ-bond cleavage which operates by an alternative mechanism was reported in 2002 by Bergman and Brookhart (Scheme 2).[3] Supported by kinetic studies, and isolated intermediates, it was shown that the mechanism of this transformation involves the silylmetallation of an organonitrile. The resulting η²-imminoacyl rhodium complex, **1b**, can readily undergo C-C bond-cleaving retromigratory insertion to generate rhodium isocyanide complex **1c**. While the process developed by Bergman and Brookhart was stoichiometric in nature, it paved the way for a catalytic variant, reported in 2006 by Chatani and Tobisu.[4] They demonstrated that hexamethyldisilane (Me_3Si-$SiMe_3$) could be used to convert aryl nitriles into the corresponding aryl silanes (Ar-$SiMe_3$; Scheme 3) using a commercially available and robust precatalyst ($[Rh(COD)Cl]_2$), albeit at high temperatures, *vide infra*. Analogous processes, generating arenes and aryl boronic ester products, using silane[5] and diborane[6] reagents, respectively, were later developed by the same research group. The reactions

were proposed to proceed via similar or related mechanisms. In particular, the decyanative borylation of aryl nitriles via the formation of imminoacyl intermediates has been supported both by computation,[7] and stoichiometric studies performed by Esteruelas and coworkers.[8] To the best of our knowledge however, the kinetics of catalyst activation and turnover of this fascinating class of reactions have not been reported.

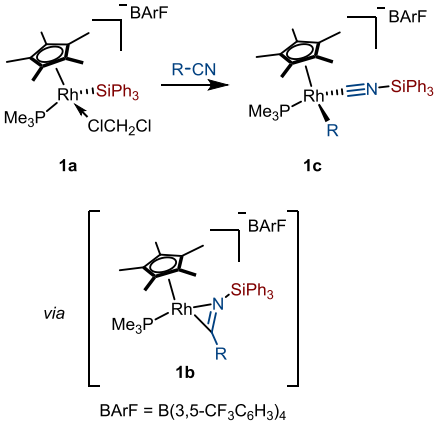

Scheme 2. Silyl Mediated C-C Bond Cleavage.

We were drawn to the silylation of aryl nitriles, a process that uses a simple homogeneous catalyst system, and proceeds in the absence of base or any extraneous additives or ligands. The aryl silane products are versatile reagents in organic chemistry. They are stable to both air and moisture, undergo transmetalation to late transition metals,[9] and have recently proven to be very effective coupling partners in gold-catalyzed oxidative arylation of alkenes[10]and arenes.[11] The preparation of $ArSiR_3$ reagents by Chatani-Tobisu silylation (Scheme 3) provides an appealing alternative to the more common strategies, e.g. lithiation / silylation.

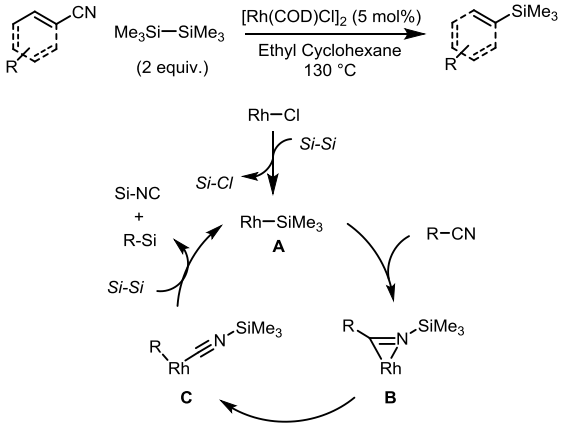

Scheme 3. Chatani-Tobisu Silylation

We were thus intrigued as to why the procedure has not been more widely adopted. Features that may be in part responsible for this are the relatively high reaction temperatures (130-150 °C) as well as high catalyst loadings and long reaction times. Herein we report on an *in-situ* study of the Chatani-Tobisu decyanative silylation, conducted to elucidate the mechanistic origins of the limiting features of the reaction. As described below, an array of kinetic phenomena that mask what is an underlying efficient catalytic process have been elucidated, these include pre-catalyst auto-induction, reagent inhibition and catalyst auto-inhibition.

Discussion

Although relatively few details on the mechanism were provided in the original reports,[4] preliminary ^{29}Si NMR studies did identify that Me_3SiCl was generated from stoichiometric reaction of the $[Rh(COD)Cl]_2$ precatalyst with $Me_3Si\text{-}SiMe_3$.[4b] This process was proposed to generate a rhodium silyl species **A** (Scheme 3) which could then catalyze conversion of ArCN to $ArSiMe_3$ and the isonitrile $Me_3Si\text{-}NC$, via a Bergman-Brookhart type mechanism[3] (Scheme 2). The resulting isonitrile ($Me_3Si\text{-}NC$) was proposed to isomerize, off metal, to its nitrile isomer ($Me_3Si\text{-}CN$). The latter species was detected in the reaction mixture at the end of the reaction, and identified by trapping with acetophenone / I_2.[4b] To effect turnover, the catalyst must cleave the Si-Si bond in the bulky and relatively unreactive hexaalkyldisilane,[12] however, details on the identity of the catalyst, including ligation, and the oxidation state(s) of intermediates remained elusive.

1. Selection of Conditions for In-situ Analysis. We chose the reaction of 4-fluorobenzonitrile, **2** with hexamethyldisilane, **3** in mesitylene, catalyzed by $[Rh(COD)Cl]_2$ for detailed study. Conducting the reaction under the reported conditions (2.0 M **2**; 4.0 M **3**; 5 mol % Rh; sealed tube, 130 °C)[4a] resulted in >95% conversion of **2** over a period of 18h, and the generation of 84% **4** (^{19}F NMR) and Me_3SiCN (^{29}Si NMR). However, the high concentrations of reactants (6 M), and the resulting viscosity of the reaction medium, led to poor quality NMR spectra. By reducing the concentrations 20-fold, the process could be cleanly monitored *in-situ* by ^{19}F NMR at 130 °C. On further investigation, the reaction profile was found to be identical to that obtained by periodic heating, with intermittent analysis at standard NMR spectrometer probe temperatures (27 °C). This quasi-*in-situ* monitoring procedure proved much more efficient, as it allowed a series of reactions to be analyzed in parallel by NMR.

2 Identification of Three Phases of Turnover. Using this quasi-*in-situ* monitoring technique, a number of key features emerged, Fig 1A. The reaction proceeds in three distinct phases: an induction period is followed by a short period of accelerating turnover (the 'burst-phase'), which in turn is followed by a prolonged period with marked and progressive reduction in turnover rate. Overall, this

results in an elongated sigmoidal temporal product concentration profile, and complete conversion of **2** requires 7 days to reach >90% conversion.

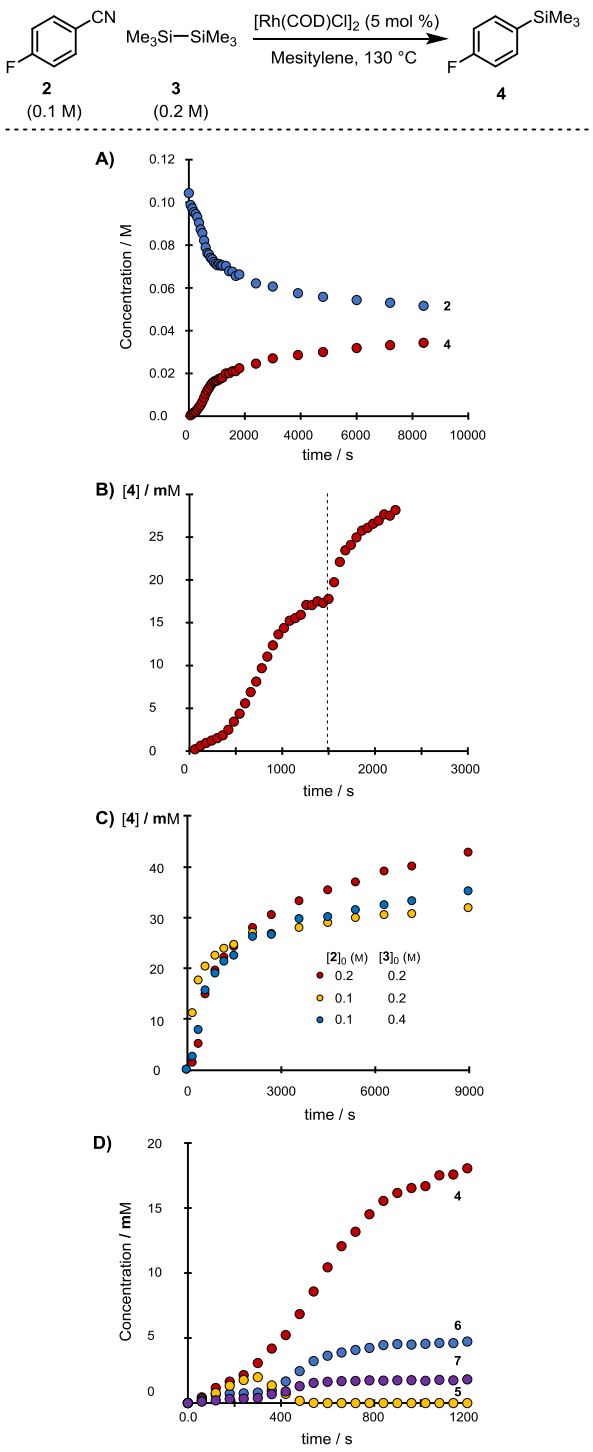

Figure 1. A) Typical temporal reaction concentration profile. B) Effect of additional $[Rh(COD)Cl]_2$ (5 mol%) added at 1500 s. C) Effect of initial concentrations on length of induction. D) Comparison of temporal concentration profile of intermediates associated with pre-catalyst activation (**5**, **6**, **7**) with reaction product **4**.

The total reaction time contrasts with the burst-phase where 20% conversion of **2** occurs in just 20 mins; features that are indicative of powerful catalyst inhibition during reaction. Addition of a second batch of pre-catalyst (5 mol %) in the early stages of inhibition resulted in a second burst-phase, notably shorter, and *without* an induction period (Fig. 1B).

Further investigation revealed that the length of the induction period[13] depends on the initial concentrations of both the aryl nitrile **2** and the disilane **3**, the former lengthening it, the latter shortening it, Fig 1C.[13] During induction, two Ar-derived species (**5** and **6**) are generated. Their temporal concentration profiles, Fig 1D, suggest that they are generated sequentially (**2**→**5**→**6**) with $[\mathbf{6}]_{max}$ = ~0.5$[Rh]_0$. ^{13}C NMR analysis using ^{13}CN-labelled substrate ($^{13}C_1$-**2**) indicated that both **5** and **6** retain the cyanide-derived carbon from **2**, with chemical shifts (δ_C = 169.2, 160.1 ppm (**5**) and 165.0, 171.2 ppm (**6**)) indicative of Ar-C(Y)=X type structures, e.g. where Y = Cl, and X = N-$SiMe_3$. However, both species proved highly-reactive and evaded isolation. In addition to **5** and **6**, fluorobenzene (**7**, 1.8 %) is generated as the burst-phase ensues, presumably via protoderhodation.[14] The proton-source was not identified, and **7** was always generated in trace levels, despite assembly of reactions in a N_2-filled glove-box, using rigorously-dried reactants, solvents and catalyst.

Similar-shaped sigmoidal reaction profiles were observed at higher concentrations of both **2** and **3** (Fig. 1C). However, although higher concentrations of **3** (0.4 M) reduce the length of the induction period and lead to higher rates in the burst-phase, it also causes slower rates of turnover during the inhibition-phase. In contrast, higher concentrations of **2** result in longer induction but faster turnover during inhibition, vide infra. The transitions between induction, burst-phase and inhibition also gave characteristic color changes: the homogeneous yellow pre-catalyst solution turns intensely-orange/red as the burst-phase ensues, and then yellow/brown as the inhibition-phase is established; indicative of distinct changes in Rh-speciation.

3. Catalyst Inhibition versus Turnover Number. Pathways for catalyst decomposition and inhibition are often overlooked in reaction development, but understanding such processes inform the design of improved catalyst performance, in particular the turnover number.[15] A key insight to the inhibition occurring in the Chatani-Tobisu silylation came from analysis of the transition from burst-phase to inhibition-phase as a function of pre-catalyst concentration, Figure 2. By normalizing the reaction profiles by catalyst turnover number, it became evident that the onset of inhibition occurs after consumption of 3.0±0.5 molecules of aryl nitrile per rhodium. Analysis by ^{29}Si NMR indicated that the Me_3SiCN co-product is generated

in increasing concentration through the inhibition-phase, but cannot be detected in solution during induction or the burst-phase. At no stage in the reaction was solution-phase isonitrile (Me_3Si-NC) detected (^{29}Si NMR), and collectively the data suggests that three molecules of Me_3SiCN/NC accumulate during the burst phase of the reaction, but remain in a rhodium-bound state.

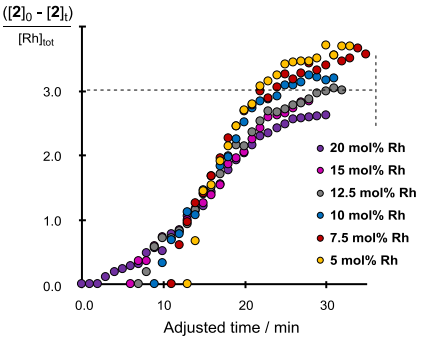

Figure 2. Consumption of **2**, normalized by total rhodium concentration, at different $[Rh(COD)Cl]_2$ precatalyst loadings.

4. Identification of Rh-isonitrile Complexes. Further *in-situ* ^{29}Si NMR analysis, after the onset of inhibition revealed that in addition to Me_3SiCl, Me_3Si-O-$SiMe_3$, Me_3Si-$SiMe_3$ (**3**), Me_3SiCN and $ArSiMe_3$ (**4**), two species (**8** / **9**) are also present, but at low concentrations. The net concentration of **8** + **9** is proportional to the rhodium-catalyst loading, indicative that they are rhodium complexes. Their relative abundance (**8** / **9**) is dependent on the reactant (ArCN **2**/ disilane **3**) proportions, **8** being favored by higher concentrations of arylnitrile, $[\mathbf{2}]_0$, Figure 3A.

Complex **9** displays more informative spectral data, consistent with three silicon environments (two isochronous). There are two doublets at δ = 2.7 and −2.7 ppm, with rhodium-couplings ($^1J_{Si\text{-}Rh}$ = 19.2, and 19.7 Hz, respectively) indicative of Rh-$SiMe_3$ moieties, Figure 3B. When ^{13}C-nitrile labelled 4-fluorobenzonitrile ($^{13}C_1$-**2**) is employed, the upper-field doublet gains an additional quartet coupling (δ = −2.7 ppm, $^2J_{Si\text{-}C}$ = 5.1 Hz), the other doublet δ = 2.7 ppm becoming a non-resolved multiplet, Figure 3C. The second pair of silicon environments are present as singlets at δ = 2.2 ppm, which become doublets ($^1J_{Si\text{-}N}$ = 5.2 Hz) when ^{15}N-labelled 4-fluorobenzonitrile (^{15}N-**2**) is employed, Figure 3D.

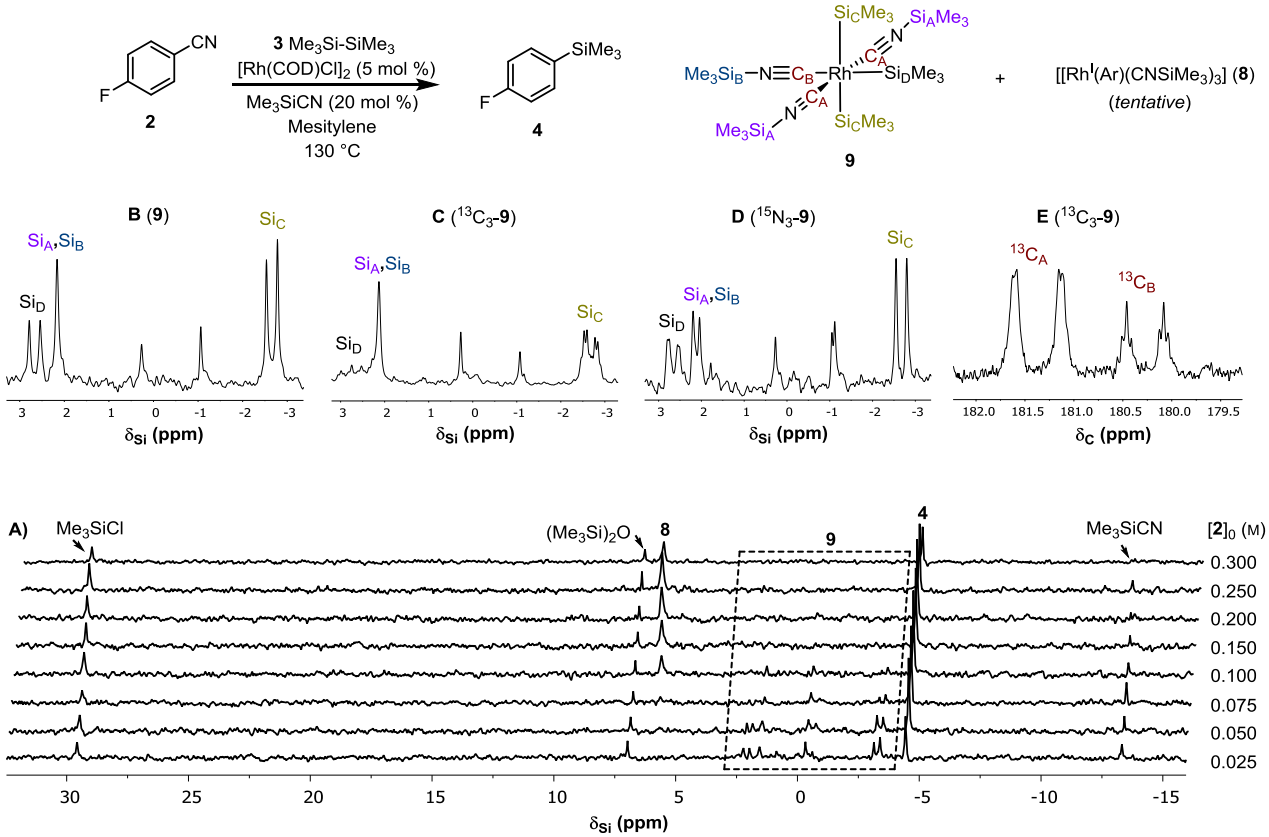

Figure 3. In situ analysis by ^{29}Si NMR (80 MHz) and $^{13}C\{^1H\}$ NMR (101 MHz) of Rh-catalyzed reactions ($[Rh]_{tot}$ = 0.01 M) of **2** (0.025 to 0.3 M) with **3** (0.1 M) in h_{12}-mesitylene at 300 K, during the inhibition phase. A) ^{29}Si NMR spectra of reactions conducted with varying initial concentrations of ArCN (**2**); signal for **3** (–20 ppm) not shown. B) reference ^{29}Si NMR sub-spectrum of **9** generated from unlabeled **2**. C) ^{29}Si NMR sub-spectrum of $^{13}C_3$-**9** generated from ^{13}C-**2**. D) ^{29}Si NMR sub-spectrum, reaction $^{15}N_3$-**9** generated from ^{15}N-**2**. E) $^{13}C\{^1H\}$ NMR sub-spectrum of $^{13}C_3$-**9** generated from ^{13}C-**2**.

Complex **8** displays the simplest ^{29}Si NMR spectral data, a slightly broadened singlet (δ = 6.0 ppm), assumed to arise from a Me_3Si moiety, and is the hardest to identify. The lack of any evident Rh-coupling, or ^{13}C-coupling when$^{13}C_1$-**2** is employed, suggests the Me_3Si is bound to N, i.e. as an isonitrile. The generation of three molecules of $ArSiMe_3$ (**4**), Figure 2, before any of the co-product (Me_3SiCN) is detected in solution, then suggests that **8** bears *three* isonitrile ligands, ([Rh^I(X)(CNSiMe$_3$)$_3$]. Since the Cl from the [Rh(COD)Cl]$_2$ pre-catalyst emerges as Me_3SiCl during induction, and there are no signals evident for Me_3Si-Rh, (i.e. X is not Cl, or Me_3Si) a process of elimination suggests that **8** is a complex of the form as [Rh^I(Ar)(CNSiMe$_3$)$_3$], where the isonitrile ligands undergo exchange at the ^{29}Si NMR timescale; however this assignment is tentative.

The ^{13}C{^{1}H} NMR spectrum of the reaction of $^{13}C_1$-**2** during the inhibition phase displayed several downfield resonances, most notably two multiplets (δ = 180.4 and 180.3 ppm, $^1J_{Rh\text{-}C}$ = 37.7, and 46.8 Hz, $^2J_{C\text{-}C}$ = 4.7 and 3.6 Hz respectively), indicative of rhodium bound isocyanides, Figure 3E.[16] At higher conversions, additional downfield multiplets are observed in the ^{13}C{^{1}H} NMR spectrum, likely to arise from higher-order isocyanide complexes, see SI for further details. Collectively, the ^{29}Si/^{13}C NMR data are consistent with the presence of two species, a Rh(I) complex tentatively assigned as [Rh^I(Ar)(CNSiMe$_3$)$_3$] (**8**) and favored by higher concentrations of ArCN (**2**), and a Rh(III) complex (**9**) with a [*mer*-Rh^{III}(SiMe$_3$)$_3$(CNSiMe$_3$)$_3$] type structure, favored by higher concentrations of Me_3Si-$SiMe_3$ (**3**).

5. Synthesis and Activity of Rh(III)-Silyl Complex 9. To the best of our knowledge, a Rh^{III}(SiMe$_3$)$_3$ type complex has not been previously described in the literature, although complex **9** is reminiscent of iridium tris(boryl) species previously described by Marder and Westcott,[17] and Ishiyama, Miyaura and Hartwig.[18] Complex **9** was independently synthesized by the reaction of [Rh(COD)Cl]$_2$ with excess Me_3SiCN and Me_3Si-$SiMe_3$ in toluene at 130 °C in a sealed tube under N_2 (Fig. 4). The complex is highly air- and moisture-sensitive, and was analyzed *in-situ* by ^{13}C/^{29}Si NMR. All attempts to crystallize it were unsuccessful; indeed removal of the solvent, or addition of hexane resulted in the immediate precipitation of an intensely purple-colored solid, tentatively assigned as **10**, potentially in polymeric form.[19] Complex **9** reacts with 1 equivalent 4-fluorobenzonitrile **2** in the presence of **3** at 130 °C, to generate $ArSiMe_3$ **4**. With ^{13}C-labelled $^{13}C_1$-**2**, the reaction generates ^{13}C-labelled **9** with the two isonitrile sites labelled in the expected 2:1 statistical ratio, Fig. 4.

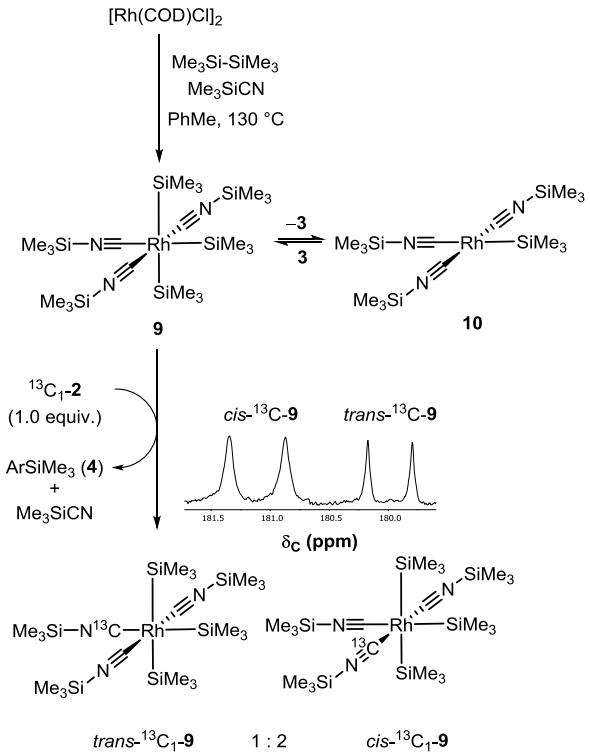

Figure 4. Synthesis and reactivity of complex **9**. After 4.5 h, there is 63% conversion of $^{13}C_1$-**2**, to generate 39% $ArSiMe_3$ **4** and 10 % fluorobenzene (**7**); ^{19}F NMR. inset shows *in situ* ^{13}C{^{1}H} NMR sub-spectrum (isonitrile region) after approximately 20% conversion of **9** to $^{13}C_1$-**9**.

6. Catalyst Inhibition by Me_3SiCN. The preferential coordination of Me_3SiCN to electron rich transition metals via its isonitrile isomer has been reported.[20] Moreover, the isoelectronic ligand carbon monoxide is a known catalyst inhibitor in rhodium-catalyzed decarbonylation and hydroacylation.[21] We thus tested the effect of *exogenous* Me_3SiCN on the Chatani-Tobisu silylation. When 10 mol % of Me_3SiCN is added to the reaction during the burst-phase, the early onset of inhibition is observed (Fig. 5). With 20 mol %, there is a near-immediate transition from the burst-phase to the inhibition-phase. Analysis of the reaction mixtures by ^{29}Si NMR spectroscopy indicated that complex **9** forms immediately after addition of the Me_3SiCN. Addition of 20 mol % of the isosteric ligand tertbutyl isocyanide (*t*BuNC) resulted in immediate inhibition of turnover, suggesting that isonitrile-nitrile isomerization may be necessary for catalyst turnover, *vide infra*.

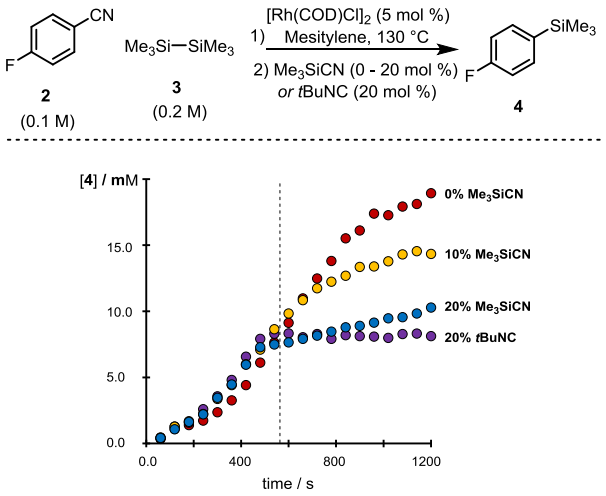

Figure 5. The effect of exogenous Me_3SiCN, added at t = 480 seconds, the approximate mid-point of the 'burst-phase', on the evolution of the Rh-catalyzed reaction of **2** with **3**.

7. Pre-catalyst Induction by Me_3SiCN. A remarkable difference in outcome is observed when Me_3SiCN is present at the *start* of the reaction. With just 10 mol % exogenous Me_3SiCN, the usual induction period is completely bypassed, allowing direct entry into the burst-phase of the reaction (Fig. 6). Moreover, the unidentified species **5** and **6** associated with the normally slow induction process, are absent. With increasing loadings of Me_3SiCN, the burst-phase is also bypassed, and the inhibition phase entered directly. However, catalyst turnover becomes disproportionately inhibited when >40 mol % of Me_3SiCN is added, suggesting that in addition to acceleration of pre-catalyst induction, there is a competing Me_3SiCN-induced pre-catalyst degradation.

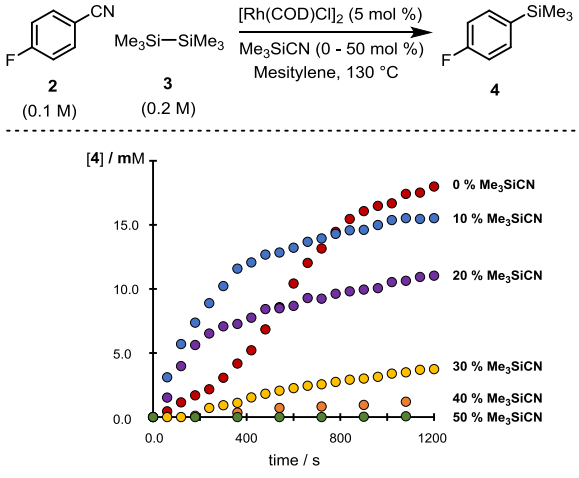

Figure 6. The effect of exogenous Me_3SiCN, added at t = 0, on the evolution of the Rh-catalyzed reaction of **2** with **3**.

The profound reduction in the pre-catalyst induction period by Me_3SiCN explains why the normal reaction profile (Figure 1A) displays an accelerating burst-phase: *endogenous* Me_3SiCN arising from slow initial turnover effects pre-catalyst auto-induction, Scheme 4. Alkyl isocyanide ligands accelerate Pd-catalyzed activation of Si-Si bonds, an effect ascribed to the small steric environment that they imposed at the metal center.[12,22] To further explore this aspect, 10 mol % *t*BuNC was tested, and analogously to Me_3SiCN, this effects rapid pre-catalyst induction, even at low hexamethyldisilane concentrations, Fig 7. The isomeric nitrile (*t*BuCN, 10 mol%) caused no significant change in the evolution of the reaction (induction, burst phase, inhibition), see SI, indicative that it is unable to isomerize to *t*BuNC under the reaction conditions.

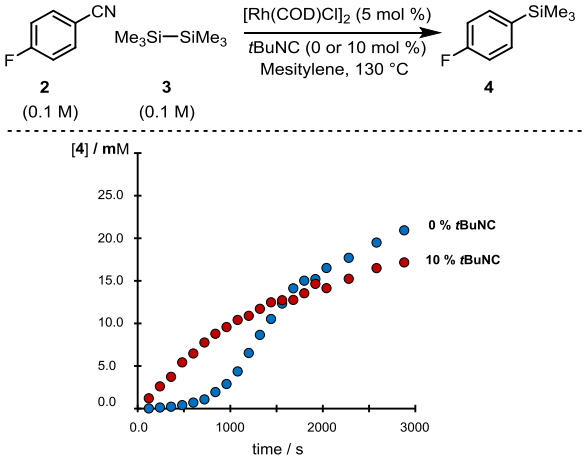

Figure 7. The effect of *t*BuNC (0.01 M, 10 mol %) at t = 0, on the evolution of the Rh-catalyzed reaction of **2** with **3**.

In-situ ^{29}Si NMR analysis of the $[Rh(COD)Cl]_2$ / **3** pre-catalyst mixture confirmed that Me_3SiCl (δ= 30 ppm), the co-product of catalyst activation, is generated *at room temperature* on addition of exogenous Me_3SiCN. Up to 30 mol % of Me_3SiCN can be added before *free* Me_3SiCN is detected, and ^1H NMR analysis shows that the COD ligand is fully liberated from Rh. All of the above suggests that the induction and auto-induction processes both lead to isonitrile-ligated Rh-silyl complexes (L = Me_3SiNC, Scheme 4).

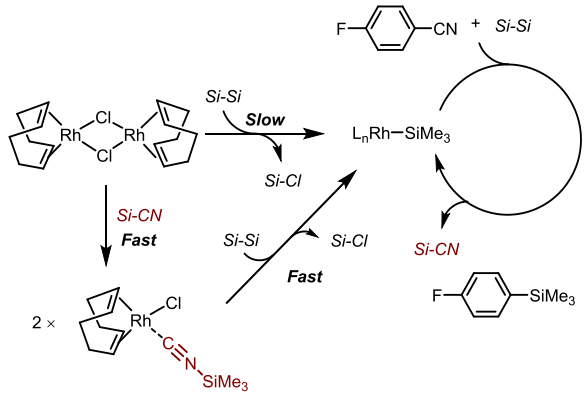

Scheme 4. Pre-catalyst Induction and Auto-induction.

8. Kinetic Analysis of the Inhibition-Phase. With a method in hand to bypass induction and the associated side-products (**5**, **6**), the kinetics of turnover during the major phase of the reaction could be efficiently explored. The initial rate of product generation ($ArSiMe_3$, **4**) was analyzed by ^{19}F NMR during the first 30±10 minutes of turnover in the inhibition-phase, with systematic variation in the initial concentrations of the $[Rh(COD)Cl]_2$ pre-catalyst, the arylnitrile **2**, and disilane **3**, (Figures 8A, 8B, 8C respectively).

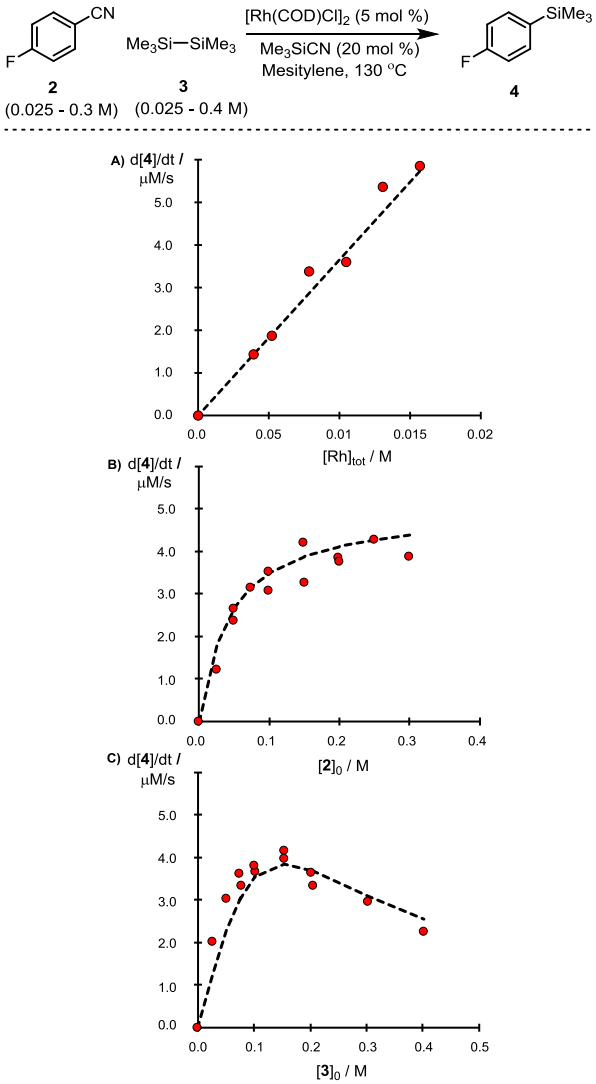

Figure 8. Initial rate of product (**4**) generation, during the inhibition-phase, as a function of initial concentration. Conditions: A. $[Rh]_{tot}$ varied, $[\mathbf{2}]_0$ = 0.1 M; $[\mathbf{3}]_0$ = 0.2 M; B. [**2**] varied, $[Rh]_{tot}$ = 0.01 M; $[\mathbf{3}]_0$ = 0.2 M; C. [**3**] varied, $[Rh]_{tot}$ = 0.01 M; $[\mathbf{2}]_0$ = 0.1 M. Data: filled circles. Dashed line, initial rate from steady-state model shown Scheme 5, where $K[Me_3SiCN]$ = 4.3 M^{-1} and $k_3 = 4.9 \times 10^{-3}$ $M^{-1}s^{-1}$.

Three distinct kinetic dependencies are observed. The simplest is that in Figure 8A, where the rate is directly proportional to the $[Rh]_0$ concentration, indicative of a monomeric catalyst system, nominally mononuclear ($[Rh]_1$). The initial rate dependency on arylnitrile, Figure 8B, displays a classic saturation profile, i.e. tending towards independence of $[\mathbf{2}]_0$, at higher concentrations. The disilane gave the most complex profile, Figure 8C; the rate increasing with $[\mathbf{3}]_0$ at lower concentrations, before reaching a threshold in $[\mathbf{3}]_0$, above which the rate begins to decrease. The profile is indicative of competitive inhibition by the reagent (disilane **3**).[23] There was no evidence for product inhibition ($ArSiMe_3$), as confirmed by control experiments $[\mathbf{4}]_0$ = 0.05 M (50 mol %), see SI.

The overall kinetics can be accounted for by a steady-state rate equation[24] based on the simple model shown in Scheme 5. Whilst individual rate constants cannot be explicitly solved, i.e. there are numerous values that collectively provide an equally good fit to the data, the model does allow for a scenario in which there are two dominant catalyst species, **8** and **9**. In such a model, increasing ArCN (**2**) concentration favors equilibrium K_1, thus increasing the rate of generation of complex **8**, via k_2. In contrast, increasing disilane (**3**) concentration accelerates the generation of product (**4**) by depleting (k_3) **8**, but also inhibits turnover by reversible generation (K_4) of **9**. Under these conditions, concentrations of **2** / **3** that distribute the rhodium equally between **8** and **9** facilitate the most efficient turnover; for $[\mathbf{2}]_0$ = 0.1 M, this condition is satisfied when $[\mathbf{3}]_0$ = 0.15 M, Figure 8C.

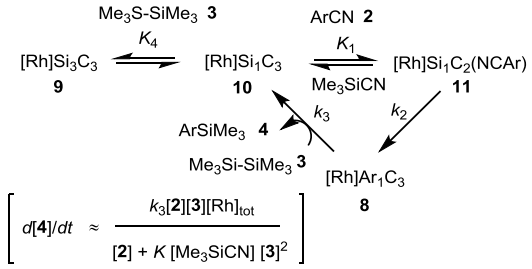

Scheme 5. Steady-State Model for Turnover

9. Mechanism of Chatani-Tobisu Decyanative Silylation. Based on our observations, and previous reports,[3-4] we propose the overarching mechanism depicted in Figure 9 to be the major pathway for induction and turnover in Chatani-Tobisu decyanative silylation reaction. The process has three main phases (I-III).

In the induction-phase (I), the pre-catalyst undergoes very slow reaction with disilane (**3**) to generate Me_3Si-Cl and small quantities of a rhodium-silyl complex. Increasing disilane concentration increases the rate, shortening the induction period. During induction, the COD ligand is also displaced, and presumably replaced by aryl nitrile (**2**) ligands. The resulting Rh(I) complex can then induce what is in effect a nitrile-isonitrile isomerization (see inset to Figure 9) to generate rhodium aryl complex **8**, bearing

a nascent Me_3Si-NC ligand. Reaction of **8** with disilane (**3**) generates the Ar-$SiMe_3$ product (**4**) and rhodium silyl complex **10**. A second nitrile-isonitrile isomerization, followed by coordination of aryl nitrile (**2**), completes the catalytic cycle and liberates Me_3Si-CN.

The second stage of turnover, the 'burst-phase' (II), involves auto-induction. Coordination of Me_3Si-CN to the precatalyst accelerates its reaction with disilane (**3**) to generate Me_3Si-Cl and active Rh-silyl species; this effect is counteracted by increasing concentration of aryl nitrile (**2**), lengthening the period required to enter the burst-phase. As more catalyst becomes activated, the rate of generation of Me_3Si-CN rises, as does the rate of pre-catalyst activation, until all of the rhodium is 'on-cycle'.

The third stage of turnover, the 'inhibition-phase' (III), involves auto-inhibition, and is entered after three full turnovers of catalyst. At this stage, rhodium complex **8** has been saturated with Me_3Si-isonitrile ligands. Turnover requires Me_3Si-nitrile-displacement by aryl nitrile (**2**); progressive turnovers reduce the concentration of **2** and increase the concentration of Me_3Si-CN, leading to progressive decrease in turnover rate. Exogenous Me_3Si-CN induces all of the above effects. The disilane concentration also impacts on the rate of turnover during phase III. Increasing disilane **3** concentration accelerates product-generation from what is tentatively assigned as a rhodium aryl complex **8**, presumably via a Rh(III)trisilyl intermediate analogous to **9**. However, generation of **9** moves rhodium off-cycle, leading to reduction in overall turnover rate. The relative proportions of the major resting states, **8** and **9,** and thus turnover rate, are thus dictated by the concentrations of **2** and **3**.

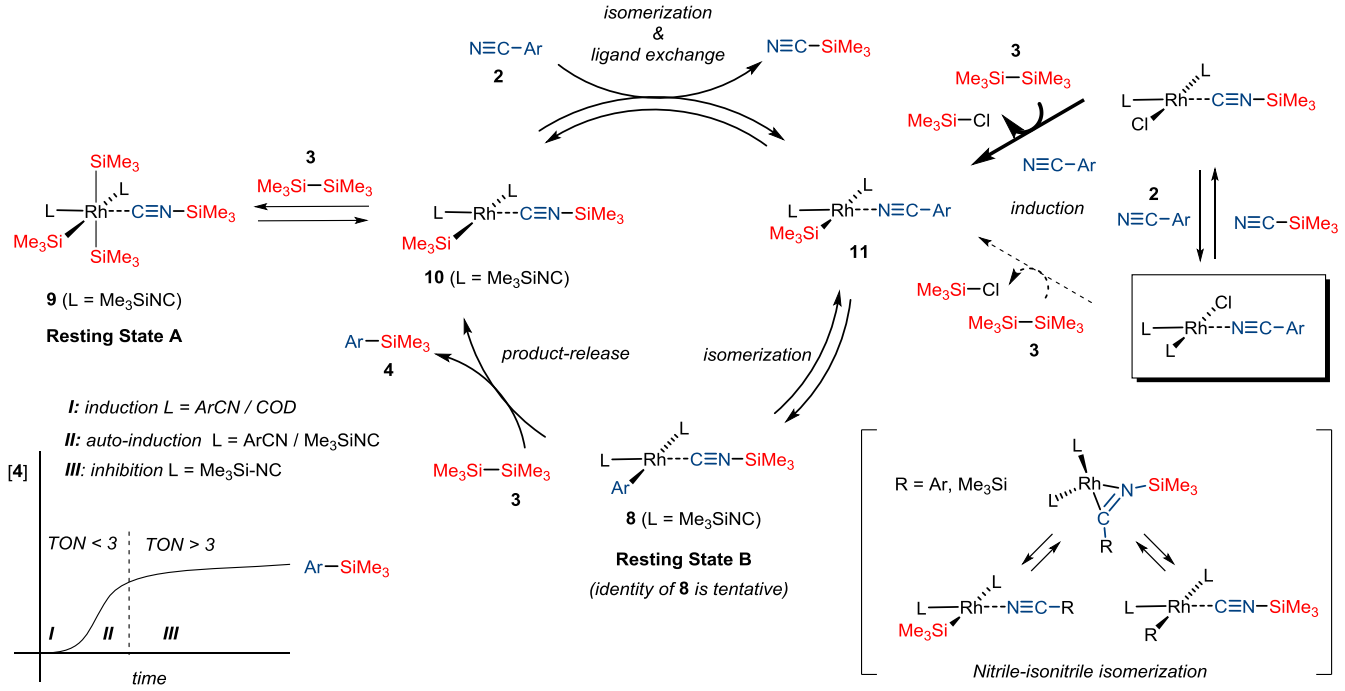

Figure 9. Mechanisms for induction (phase I), turnover (phase II) and inhibition (phase III) in Chatani-Tobisu Decyanative Silylation of aryl nitriles (**2**) by disilane reagent **3**. Inset to lower left shows schematic temporal concentration profiles for the three distinct phases. The inset in the lower right shows the generic mechanism for nitrile-isonitrile isomerization with accompanying exchange of ligands (R / Me_3Si) bound to Rh.

Conclusions

The Chatani-Tobisu rhodium catalysed decyanative silylation of aryl nitriles with disilanes[4] is a reaction with substantial but as yet unrealized potential for application. Herein we have demonstrated that the process displays a number of kinetic phenomena that are rarely reported in homogenous catalysis. Key features include auto-induction, reagent-inhibition, and auto-inhibition. Whilst the cycle presented in Figure 9 is simplified and contains a number of 'telescoped' steps, it accounts for all of the spectroscopic (NMR) observations and kinetic phenomena detailed above. In particular it explains the origins of the three phases of turnover: induction (I), burst-phase (II), and inhibition (III). We have also detected (by $^{29}Si/^{13}C$ NMR) two major resting states in the reaction. One is tentatively assigned as [$Rh^{I}(Ar)(CNSiMe_3)_3$] (**8**),[25] the other, a [*mer*-$Rh^{III}(SiMe_3)_3(CNSiMe_3)_3$] complex (**9**) has been independently synthesized, allowing demonstration of its relevance to the catalytic cycle, albeit as an off-cycle intermediate.

All of the components in the reaction, other than the arylsilane product (**4**) play conflicting roles in the overall

process: the aryl nitrile substrate (**2**) inhibits the induction (I), and burst-phase (II), but accelerates turnover during inhibition (III), within the limits of saturation (Figure 8B). The silane reagent (**3**) accelerates induction (I), the burst-phase (II), and turnover during inhibition (III), within the limits of competitive inhibition, becoming an inhibitor at high concentrations (Figure 8C). The Me_3SiCN co-product accelerates induction (I), thus leading to the burst-phase (II), but it inhibits turnover during phase (III) by competing with aryl nitrile **2** as a ligand for rhodium. Reactions in which substrates and products have such contradictory roles are rare in the literature. The analysis indicates that optimum catalyst performance will be achieved with [**3**] / [**2**] ratios that depend on the absolute concentration of **2**; in other words under some conditions, substoichiometric quantities of **3** will provide maximum rate. Reactions conducted at twenty-fold higher initial concentrations of reactants **2** and **3** (both 2 M) employing 1 mol% Rh, with 2 mol% Me_3SiCN to bypass induction, and analyzed by the quasi-*in-situ* ^{19}F NMR monitoring procedure, also displayed a burst phase followed by progressive inhibition. As the initial concentration of silane (**3**) is reduced to 1 M then 0.7 M, the rate of turnover in the burst phase increased, consistent with silane **3** acting as an inhibitor under the normal conditions employed for synthesis, see SI.

It is also of note that the proposed mechanism requires no off-metal nitrile-isonitrile isomerization processes, and thus no free Me_3SiNC isonitrile in solution, as is observed experimentally. The mechanism also explains the dramatic effects observed when *t*BuNC is added to the reaction (Figure 5): the burst-phase is directly entered, and if *t*BuNC is ineffective in nitrile-isonitrile isomerization (as suggested by the lack of inhibition on addition of *t*BuCN), it will remain ligated as its *C*-bound isomer, undergoing much slower displacement by aryl nitrile (**2**) and thus very slow turnover. The effect of isocyanides on the activation of disilanes, to the best of our knowledge has not been previously reported in rhodium catalysis.

The results presented may be viewed as a cautionary study on the importance of mechanistic understanding in reaction development. The study predicts that i) sequestration of the Me_3SiCN co-product from the reaction mixture; ii) use of a rhodium silyl precatalyst, and iii) careful selection of absolute and relative reactant (**2**/**3**) concentrations, will together lead to substantial increases in the efficiency and thus broader application of Chatani-Tobisu decyanative silylation.[4]

AUTHOR INFORMATION

Corresponding Author

*Guy.Lloyd-Jones@ed.ac.uk

Notes

The authors declare no competing financial interest.

ASSOCIATED CONTENT

Supporting Information. NMR spectra, kinetic analyses, synthesis of reactants. This material is available free of charge via the Internet at http://pubs.acs.org.

ACKNOWLEDGMENT

The research leading to these results received funding from the European Research Council under the European Union's Seventh Framework Programme (FP7/2007−2013)/ERC Grant Agreement 340163, and the National Science and Engineering Research Council of Canada (NSERC, PDF-471815-2015).

REFERENCES

(1) (a) Rybtchinski, B.; Milstein, D. Metal Insertion into C−C Bonds in Solution. *Angew. Chem. Int. Ed.* **1999**, *38*, 870–883. (b) Murakami, M; Matsuda, T. Metal-Catalysed Cleavage of Carbon–Carbon Bonds. *Chem. Commun*. **2011**, *47*, 1100–1105 (c) Chen, F.; Wang, T.; Jiao, N. Recent Advances in Transition-Metal-Catalyzed Functionalization of Unstrained Carbon–Carbon Bonds. *Chem. Rev.* **2014**, *114*, 8613–8661. (d) Souillart, L.; Cramer, N. Catalytic C–C Bond Activations via Oxidative Addition to Transition Metals. *Chem. Rev.* **2015**, *115*, 9410–9464. (e) Murakami, M; Ishida, N. Potential of Metal-Catalyzed C–C Single Bond Cleavage for Organic Synthesis. *J. Am. Chem. Soc.* **2016**, *138*, 13759-13769.

(2) Tobisu, M.; Chatani, N. Catalytic Reactions Involving the Cleavage of Carbon–Cyano and Carbon–Carbon Triple Bonds. *Chem. Soc. Rev.* **2008**, *37*, 300−307.

(3) (a) Taw, F. L.; White, P. S.; Bergman, R. G.; Brookhart, M. Carbon−Carbon Bond Activation of R−CN (R = Me, Ar, ^{i}Pr, ^{t}Bu) Using a Cationic Rh(III) Complex. *J. Am. Chem. Soc.* **2002**, *124*, 4192−4193. (b) Taw, F. L.; Mueller, A. H.; Bergman, R. G.; Brookhart, M. A Mechanistic Investigation of the Carbon−Carbon Bond Cleavage of Aryl and Alkyl Cyanides Using a Cationic Rh(III) Silyl Complex. *J. Am. Chem. Soc.* **2003**, *125*, 9808−9813. For a computational study of this mechanism see: (c) Zhang. S. L.; Huang, L.; Bie, W.-F. Mechanism for Activation of the C−CN Bond of Nitriles by a Cationic CpRhIII−Silyl Complex: A Systematic DFT Study. *Organometallics* **2014**, *33*, 3030−3039.

(4) (a) Tobisu, M.; Kita, Y.; Chatani, N. Rh(I)-Catalyzed Silylation of Aryl and Alkenyl Cyanides Involving the Cleavage of C−C and Si−Si Bonds. *J. Am. Chem. Soc.* **2006**, *128*, 8152−8153. (b) Tobisu, M.; Kita, Y.; Ano, Y.; Chatani, N. Rhodium-Catalyzed Silylation and Intramolecular Arylation of Nitriles via the Silicon-Assisted Cleavage of Carbon−Cyano Bonds. *J. Am. Chem. Soc.* **2008**, *130*, 15982−15989. (c) Kita, Y.; Tobisu, M.; Chatani, N. Rhodium-Catalyzed Carbon−Cyano Cleavage Reactions Using Organosilicon Reagents. *J. Synth. Org. Chem. Jpn.* **2010**, *68*, 8−18.

(5) Tobisu, M.; Nakamura, R.; Kita, Y.; Chatani, N. Rhodium-Catalyzed Reductive Cleavage of Carbon−Cyano Bonds with Hydrosilane: A Catalytic Protocol for Removal of Cyano Groups. *J. Am. Chem. Soc.* **2009**, *131*, 3174−3175.

(6) Tobisu, M.; Kinuta, H.; Kita, Y.; Rémond, E.; Chatani, N. Rhodium(I)-Catalyzed Borylation of Nitriles through the Cleavage of Carbon–Cyano Bonds. *J. Am. Chem. Soc.* **2012**, *134*, 115−118.

(7) (a) Jiang, Y.-Y.; Yu, H.-Z.; Fu, Y. Mechanistic Study of Borylation of Nitriles Catalyzed by Rh–B and Ir–B Complexes via C–CN Bond Activation. *Organometallics* **2013**, *32*, 926−936. (b) Kinuta, H.; Takahashi, H.; Tobisu, M.; Mori, S.; Chatani, N. Theoretical Studies of Rhodium-Catalyzed Borylation of Nitriles through Cleavage of Carbon–Cyano Bonds. *Bull. Chem. Soc. Jpn.* **2014**, *87*, 655−669.

(8) Esteruelas, M. A.; Oliván, M.; Vélez, A. Conclusive Evidence on the Mechanism of the Rhodium-Mediated Decyanative Borylation. *J. Am. Chem. Soc.* **2015**, *137*, 12321−12329.

(9) Hatanaka, Y.; Fukushima, S.; Hiyama, T. Selective Synthesis of Unsymmetrical Biaryls via Palladium-Catalyzed Cross-Coupling of Arylfluorosilanes with Aryl Iodides. *Chem. Lett.* **1989**, *18*, 1711–1714; b) Hatanaka, Y.; Hiyama, T. Highly Selective Cross-Coupling Reactions of Organosilicon Compounds Mediated by Fluoride Ion and a Palladium Catalyst. *Synlett* **1991**, 845–853; c) Denmark, S. E.; Regens, C. S. Palladium-Catalyzed Cross-Coupling Reactions of Organosilanols and Their Salts: Practical Alternatives to Boron- and Tin-Based Methods. *Acc. Chem. Res.* **2008**, *41*, 1486–1499; d) Denmark, S. E.; Ambrosi, A. Why You Really Should Consider Using Palladium-Catalyzed Cross-Coupling of Silanols and Silanolates. *Org. Process Res. Dev.* **2015**, *19*, 982-994; e) Tamao, K.; Kobayashi, K.; Ito, Y. Palladium-Catalyzed Cross-Coupling Reaction of Alkenylalkoxysilanes with Aryl and Alkenyl Halides in the Presence of a Fluoride. *Tetrahedron Lett.* **1989**, *30*, 6051–6054; f) Komiyama, T.; Minami, Y.; Hiyama, T. Recent Advances in Transition-Metal-Catalyzed Synthetic Transformations of Organosilicon Reagents. *ACS Catal.* **2017**, 7, 631–651.

(10) (a) Ball, L. T.; Green, M.; Lloyd-Jones, G. C.; Russell, C. A. Arylsilanes: Application to Gold-Catalyzed Oxyarylation of Alkenes. *Org. Lett.* **2010**, *12*, 4724−4727. (b) Brenzovich, W. E.; Brazeau, J.-F.; Toste, F. D. Gold-Catalyzed Oxidative Coupling Reactions with Aryltrimethylsilanes. *Org. Lett.* **2010**, *12*, 4728−4731; (c) Ball, L. T.; Lloyd-Jones, G. C.; Russell, C. A. Gold-Catalysed Oxyarylation of Styrenes and Mono- and gem-Disubstituted Olefins Facilitated by an Iodine(III) Oxidant. *Chem. Eur. J.* **2012**, *18*, 2931−2937.

(11) (a) Ball, L. T.; Lloyd-Jones, G. C.; Russell, C. A. Gold-Catalyzed Direct Arylation. *Science* **2012**, *337*, 1644−1648. (b) Ball, L. T.; Lloyd-Jones, G. C.; Russell, C. A. Gold-Catalyzed Oxidative Coupling of Arylsilanes and Arenes: Origin of Selectivity and Improved Precatalyst. *J. Am. Chem. Soc.* **2014**, *136*, 254−264; (c) Hata, K.; Ito, H.; Segawa, Y.; Itami, K. Pyridylidene Ligand Facilitates Gold-Catalyzed Oxidative C–H Arylation of Heterocycles. *Beilstein J. Org. Chem.* **2015**, *11*, 2737−2746; (d) Hua, Y.; Asgari, P.; Avullala, T.; Jeon, J. Catalytic Reductive ortho-C–H Silylation of Phenols with Traceless, Versatile Acetal Directing Groups and Synthetic Applications of Dioxasilines. *J. Am. Chem. Soc.* **2016**, *138*, 7982−7991; (e) Cresswell, A. J.; Lloyd-Jones, G. C. Room-Temperature Gold-Catalysed Arylation of Heteroarenes: Complementarity to Palladium Catalysis. *Chem. Eur. J.* **2016**, *22*, 12641−12645; (f) Corrie, T. J. A.; Ball, L. T.; Russell, C. A.; Lloyd-Jones, G. C. Au-Catalyzed Biaryl Coupling To Generate 5- to 9-Membered Rings: Turnover-Limiting Reductive Elimination versus π-Complexation. *J. Am. Chem. Soc.* **2017**, *139*, 245−254; (g) Corrie, T. J. A.; Lloyd-Jones, G. C. Formal Synthesis of (±)-Allocolchicine Via Gold-Catalysed Direct Arylation: Implication of Aryl Iodine(III) Oxidant in Catalyst Deactivation Pathways. *Top. Catal.* **2017**, *60*, 570−579; (h) Robinson, M. P.; Lloyd-Jones, G. C. Au-Catalyzed Oxidative Arylation: Chelation-Induced Turnover of *ortho*-Substituted Arylsilanes. *ACS Catal.* **2018**, 8, 7484−7488.

(12) (a) Ito, Y.; Suginome, M.; Murakami, M. Palladium(II) Acetate-tert-alkyl Isocyanide as a Highly Efficient Catalyst for the Inter- and Intramolecular bis-Silylation of Carbon-Carbon Triple bonds. *J. Org. Chem.* **1991**, *56*, 1948−1951. For a recent example of Rh-catalyzed Si-Si activation see: (b) He, T.; Liu, L.-C.; Guo, L.; Li, B.; Zhang, Q.-W.; He, W. Rhodium Catalyzed Intermolecular trans-Disilylation of Alkynones with Unactivated Disilanes. *Angew. Int. Ed*. **2018**, DOI: 10.1002/anie.201804223.

(13) Induction periods were estimated by linear extrapolation of the maximum rate of generation of **4** to the time point where [**4**] = 0. The maximum rate was estimated by taking the derivative of a high-order polynomial (6^{th}) fitted to the temporal concentration data for **4**. For discussion of the commonly employed technique of taking the derivative of a high-order polynomial, and associated errors and alternative methods, see Garrett, G. E.; Mark S. Taylor, M. S. A Nonlinear Ordinary Differential Equation for Generating Graphical Rate Equations from Concentration Versus Time Data. *Top. Catal*. **2017**, *60*, 554–563.

(14) Fagnou, K.; Lautens, M. Rhodium-Catalyzed Carbon−Carbon Bond Forming Reactions of Organometallic Compounds. *Chem. Rev.* **2003**, *103*, 169−196.

(15) Crabtree, R. H. Deactivation in Homogeneous Transition Metal Catalysis: Causes, Avoidance, and Cure. *Chem. Rev.* **2015**, *115*, 127−150.

(16) Ito, H.; Kato, T.; Sawamura, M. Design and Synthesis of Isocyanide Ligands for Catalysis: Application to Rh-Catalyzed Hydrosilylation of Ketones. *Chem. Asian J.* **2007**, *2*, 1436−1446.

(17) Nguyen, P.; Blom, H. P.; Westcott, S. A.; Taylor, N. J.; Marder, T. B. Synthesis and Structures of the First Transition-Metal Tris(boryl) Complexes: Iridium Complexes (η^6-arene)Ir($BO_2C_6H_4$)$_3$. *J. Am. Chem. Soc.* **1993**, *115*, 9329−9330.

(18) Ishiyama, T.; Takagi, J.; Ishida, K.; Miyaura, N.; Anastasi, N. R.; Hartwig, J. F. Mild Iridium-Catalyzed Borylation of Arenes. High Turnover Numbers, Room Temperature Reactions, and Isolation of a Potential Intermediate. *J. Am. Chem. Soc.* **2002**, *124*, 390−391.

(19) While the purple solid, dissolves in toluene, the resulting homogeneous yellow solution does not contain **9** (^{29}Si NMR). Complex **9** is however re-generated on addition of Me_3Si-$SiMe_3$ and heating to 130 °C. The results suggest that Rh(III)-silyl **9** undergoes reversible loss of Me_3Si-$SiMe_3$ (**3**) to generate Rh(I)-complex **10**. A similar equilibrium has been reported with palladium N-heterocyclic carbene (NHC) complexes: Ansell, M. B.; Roberts, D. E.; Cloke, F. G. N.; Navarro, O.; Spencer, J. Synthesis of an [$(NHC)_2Pd(SiMe_3)_2$] Complex and Catalytic cis-Bis(silyl)ations of Alkynes with Unactivated Disilanes. *Angew. Chem. Int. Ed.* **2015**, *54*, 5578−5582.

(20) (a) Seyferth, D.; Kahlen, N. (Iso)cyanides of Silicon, Germanium and Tin as Ligands in Iron Carbonyl Complexes. *J. Am. Chem. Soc.* **1960**, *82*, 1080−1082. (b) Eisch, J. J.; Aradi, A. A.; Han, K. I. Nickel(0)-mediated Hydrocyanation and Carbonylation Reactions of Alkynes with Trimethylsilyl(iso)cyanide. *Tetrahedron Lett.* **1983**, *24*, 2073−2076.

(21) (a) Murakami, M.; Amii, H.; Ito, Y. Selective Activation of Carbon–Carbon Bonds Next to a Carbonyl Group. *Nature* **1994**, *370*, 540−541. (b) von Delius, M.; Le, C. M.; Dong, V. M.

Rhodium-Phosphoramidite Catalyzed Alkene Hydroacylation: Mechanism and Octaketide Natural Product Synthesis. *J. Am. Chem. Soc.* **2012**, *134*, 15022−15032.

(22) (a) Suginome, M.; Ito, Y. Transition-Metal-Catalyzed Additions of Silicon–Silicon and Silicon–Heteroatom Bonds to Unsaturated Organic Molecules. *Chem. Rev.* **2000**, *100*, 3221−3256. (b) Suginome, M.; Oike, H.; Shuff, P. H.; Ito, Y. Double oxidative Addition of the Si–Si and Si–Ge Bonds onto Isonitrile-platinum(0) Complexes Leading to the Formation of tetrakis(organosilyl)- and bis(organogermyl)bis(organosilyl)platinum(IV) complexes. *J. Organomet. Chem.* **1996**, *521*, 405−408. (c) Suginome, M.; Kato, Y.; Takeda, N.; Oike, H.; Ito, Y. Reactions of a Spiro Trisilane with Palladium Complexes: Synthesis and Structure of Tris(organosilyl)CpPd^{IV} and Bis(organosilyl)(μ-organosilylene)Pd$^{II}_2$ Complexes. *Organometallics* **1998**, *17*, 495−497. (d) Suginome, M.; Oike, H.; Park, S.-S.; Ito, Y. Reactions of Si–Si σ-Bonds with Bis(*t*-alkyl isocyanide)palladium(0) Complexes. Synthesis and Reactions of Cyclic Bis(organosilyl)palladium Complexes. *Bull. Chem. Soc. Jpn.* **1996**, *69*, 289−299. (e) Ansell, M. B.; Navarro, O.; Spencer, J. Transition Metal Catalyzed Element–Element' Additions to Alkynes. *Coord. Chem. Rev.* **2017**, *336*, 54–77.

(23) The inhibition is 'competitive', see: Helfferich, F. In *Kinetics of Multistep Reactions*, 2nd ed.; Green. N. Ed.; Elsevier Science: Amsterdam, 2004, Vol 40, p249.

(24) The steady-state rate equation was derived by the method of King and Altman, and then simplified by applying a limiting condition that $K_4 \gg K_1$, see SI for derivation.

(25) The intermediacy of complex **8** is consistent with the known diversion of the reaction towards alkenylation by addition of vinyl triethylsilane: Kita, Y.; Tobisu, M.; Chatani, N. Rhodium-Catalyzed Alkenylation of Nitriles via Silicon-Assisted C-CN Bond Cleavage. *Org. Lett.* **2010**, *12*, 1864−1867.

Graphical Abstract